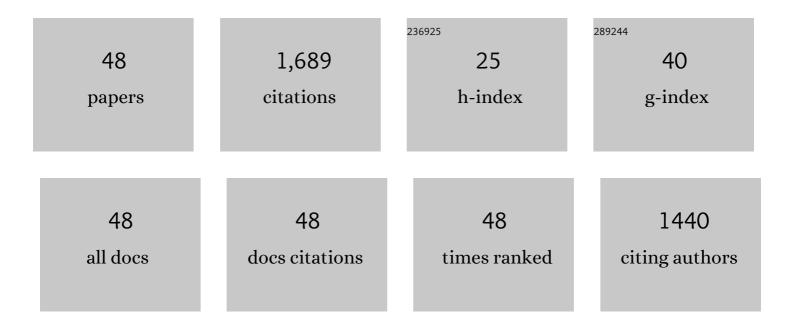
Jean Vandemeulebrouck

List of Publications by Year in descending order

Source: https://exaly.com/author-pdf/3828009/publications.pdf

Version: 2024-02-01



#	Article	IF	CITATIONS
1	Turbulence-induced bubble nucleation in hydrothermal fluids beneath Yellowstone Lake. Communications Earth & Environment, 2022, 3, .	6.8	3
2	Radon signature of CO2 flux constrains the depth of degassing: Furnas volcano (Azores, Portugal) versus Syabru-Bensi (Nepal Himalayas). Scientific Reports, 2022, 12, .	3.3	5
3	Tracking Episodes of Seismicity and Gas Transport in Campi Flegrei Caldera Through Seismic, Geophysical, and Geochemical Measurements. Seismological Research Letters, 2021, 92, 965-975.	1.9	14
4	Snapshot of a magmatic/hydrothermal system from electrical resistivity tomography and fumarolic composition, Whakaari/White Island, New Zealand. Journal of Volcanology and Geothermal Research, 2020, 400, 106909.	2.1	11
5	Editorial: Multidisciplinary Geophysical Imaging of Volcanoes. Frontiers in Earth Science, 2020, 8, .	1.8	0
6	Insight Into Campi Flegrei Caldera Unrest Through Seismic Tremor Measurements at Pisciarelli Fumarolic Field. Geochemistry, Geophysics, Geosystems, 2019, 20, 5544-5555.	2.5	26
7	Electrical resistivity tomography and time-domain induced polarization field investigations of geothermal areas at Krafla, Iceland: comparison to borehole and laboratory frequency-domain electrical observations. Geophysical Journal International, 2019, 218, 1469-1489.	2.4	32
8	Heat and Mass Transport in a Vaporâ€Dominated Hydrothermal Area in Yellowstone National Park, USA: Inferences From Magnetic, Electrical, Electromagnetic, Subsurface Temperature, and Diffuse CO ₂ Flux Measurements. Journal of Geophysical Research: Solid Earth, 2019, 124, 291-309.	3.4	14
9	3-D interpretation of short-period magnetotelluric data at Furnas Volcano, Azores Islands. Geophysical Journal International, 2018, 213, 371-386.	2.4	25
10	Anatomy of a fumarolic system inferred from a multiphysics approach. Scientific Reports, 2018, 8, 7580.	3.3	27
11	Structure of the acid hydrothermal system of Papandayan volcano, Indonesia, investigated by geophysical methods. Journal of Volcanology and Geothermal Research, 2018, 358, 77-86.	2.1	18
12	Possible deep connection between volcanic systems evidenced by sequential assimilation of geodetic data. Scientific Reports, 2018, 8, 11702.	3.3	24
13	Threeâ€Dimensional Electrical Resistivity Tomography of the Solfatara Crater (Italy): Implication for the Multiphase Flow Structure of the Shallow Hydrothermal System. Journal of Geophysical Research: Solid Earth, 2017, 122, 8749-8768.	3.4	62
14	3D ultra-high resolution seismic imaging of shallow Solfatara crater in Campi Flegrei (Italy): New insights on deep hydrothermal fluid circulation processes. Scientific Reports, 2017, 7, 3412.	3.3	35
15	Geophysical image of the hydrothermal system of Merapi volcano. Journal of Volcanology and Geothermal Research, 2017, 329, 30-40.	2.1	29
16	Hydrothermal activity and subsoil complexity: implication for degassing processes at Solfatara crater, Campi Flegrei caldera. Bulletin of Volcanology, 2017, 79, 1.	3.0	11
17	Fumarolic tremor and geochemical signals during a volcanic unrest. Geology, 2017, 45, 1131-1134.	4.4	34
18	Magmas near the critical degassing pressure drive volcanic unrest towards a critical state. Nature Communications, 2016, 7, 13712.	12.8	144

JEAN VANDEMEULEBROUCK

#	Article	IF	CITATIONS
19	A strongly heterogeneous hydrothermal area imaged by surface waves: the case of Solfatara, Campi Flegrei, Italy. Geophysical Journal International, 2016, 205, 1813-1822.	2.4	15
20	Changes in CO2 diffuse degassing induced by the passing of seismic waves. Journal of Volcanology and Geothermal Research, 2016, 320, 12-18.	2.1	15
21	Evidence of thermal-driven processes triggering the 2005–2014 unrest at Campi Flegrei caldera. Earth and Planetary Science Letters, 2015, 414, 58-67.	4.4	149
22	Volcanic Lakes. Advances in Volcanology, 2015, , 1-20.	1.1	25
23	Mapping the 2010 Merapi pyroclastic deposits using dual-polarization Synthetic Aperture Radar (SAR) data. Remote Sensing of Environment, 2015, 158, 180-192.	11.0	30
24	Relations between electrical resistivity, carbon dioxide flux, and self-potential in the shallow hydrothermal system of Solfatara (Phlegrean Fields, Italy). Journal of Volcanology and Geothermal Research, 2014, 283, 172-182.	2.1	58
25	A twoâ€magma chamber model as a source of deformation at GrÃmsvötn Volcano, Iceland. Journal of Geophysical Research: Solid Earth, 2014, 119, 4666-4683.	3.4	56
26	Eruptions at Lone Star geyser, Yellowstone National Park, USA: 2. Constraints on subsurface dynamics. Journal of Geophysical Research: Solid Earth, 2014, 119, 8688-8707.	3.4	44
27	Periodic behavior of soil CO ₂ emissions in diffuse degassing areas of the Azores archipelago: Application to seismovolcanic monitoring. Journal of Geophysical Research: Solid Earth, 2014, 119, 7578-7597.	3.4	33
28	Influence of the regional topography on the remote emplacement of hydrothermal systems with examples of Ticsani and Ubinas volcanoes, Southern Peru. Earth and Planetary Science Letters, 2013, 365, 152-164.	4.4	20
29	Eruptions at Lone Star Geyser, Yellowstone National Park, USA: 1. Energetics and eruption dynamics. Journal of Geophysical Research: Solid Earth, 2013, 118, 4048-4062.	3.4	49
30	The plumbing of Old Faithful Geyser revealed by hydrothermal tremor. Geophysical Research Letters, 2013, 40, 1989-1993.	4.0	67
31	Dyke leakage localization and hydraulic permeability estimation through self-potential and hydro-acoustic measurements: Self-potential â€abacus' diagram for hydraulic permeability estimation and uncertainty computation. Journal of Applied Geophysics, 2012, 86, 17-28.	2.1	27
32	Effects of atmospheric conditions on surface diffuse degassing. Journal of Geophysical Research, 2012, 117, .	3.3	34
33	High-resolution shallow seismic tomography of a hydrothermal area: application to the Solfatara, Pozzuoli. Geophysical Journal International, 2012, 189, 1725-1733.	2.4	20
34	Locating hydrothermal acoustic sources at Old Faithful Geyser using Matched Field Processing. Geophysical Journal International, 2011, 187, 385-393.	2.4	65
35	Electrical conductivity, ground displacement, gravity changes, and gas flow at Solfatara crater (Campi Flegrei caldera, Italy): Results from numerical modeling. Journal of Volcanology and Geothermal Research, 2011, 207, 93-105.	2.1	37
36	Application of acoustic noise and self-potential localization techniques to a buried hydrothermal vent (Waimangu Old Geyser site, New Zealand). Geophysical Journal International, 2010, 180, 883-890.	2.4	22

#	Article	IF	CITATIONS
37	Self-potential and passive seismic monitoring of hydrothermal activity: A case study at Iodine Pool, Waimangu geothermal valley, New Zealand. Journal of Volcanology and Geothermal Research, 2009, 179, 11-18.	2.1	25
38	A case study of resistivity and selfâ€potential signatures of hydrothermal instabilities, Inferno Crater Lake, Waimangu, New Zealand. Geophysical Research Letters, 2009, 36, .	4.0	39
39	The effects of hydrothermal eruptions and a tectonic earthquake on a cycling crater lake (Inferno) Tj ETQq1 1 0.7 271-275.	84314 rgB 2.1	T /Overlock 27
40	Volcano–glacier interactions on composite cones and lahar generation: Nevado del Ruiz, Colombia, case study. Annals of Glaciology, 2007, 45, 115-127.	1.4	16
41	Analogue modeling of instabilities in crater lake hydrothermal systems. Journal of Geophysical Research, 2005, 110, .	3.3	32
42	Radon anomaly in the soil of Taal volcano, the Philippines: A likely precursor of the M 7.1 Mindoro earthquake (1994). Geophysical Research Letters, 2003, 30, .	4.0	86
43	Hydroacoustic noise precursors of the 1990 eruption of Kelut Volcano, Indonesia. Journal of Volcanology and Geothermal Research, 2000, 97, 443-456.	2.1	35
44	Acoustic noise and temperature monitoring of the Crater Lake of Mount Ruapehu Volcano. Journal of Volcanology and Geothermal Research, 1996, 71, 45-51.	2.1	16
45	Thermal infrared satellite measurements of volcanic activity at Stromboli and Vulcano. Journal of Geophysical Research, 1994, 99, 9477-9485.	3.3	25
46	Implications for the thermal regime of acoustic noise measurements in Crater Lake, Mount Ruapehu, New Zealand. Bulletin of Volcanology, 1994, 56, 493-501.	3.0	8
47	Satellite monitoring of the vertical temperature profile of Lake Nyos, Cameroon. Journal of Volcanology and Geothermal Research, 1990, 42, 381-385.	2.1	8
48	Holocene paleotemperatures deduced from geothermal measurements. Palaeogeography, Palaeoclimatology, Palaeoecology, 1983, 43, 237-259.	2.3	92